Molecular dynamics investigation of dynamical heterogeneity and local structure in the supercooled liquid and glass states of Al

Maozhi Li,[1,2] Cai-Zhuang Wang,[2] Mikhail I. Mendelev,[2] and Kai-Ming Ho[2]
[1]*Department of Physics, Renmin University of China, Beijing 100872, China*
[2]*Ames Laboratory–USDOE, Iowa State University, Ames, Iowa 50011, USA*
(Received 16 December 2007; published 13 May 2008)

Molecular dynamics simulations are performed to study the structure and dynamical heterogeneity in the liquid and glass states of Al using a frequently employed embedded atom potential. While the pair correlation function of the glass and liquid states displays only minor differences, the icosahedral short-range order (ISRO) and the dynamics of the two states are very different. The ISRO is much stronger in the glass than in the liquid. It is also found that both the most mobile and the most immobile atoms in the glass state tend to form clusters, and the clusters formed by the immobile atoms are more compact. In order to investigate the local environment of each atom in the liquid and glass states, a local density is defined to characterize the local atomic packing. There is a strong correlation between the local packing density and the mobility of the atoms. These results indicate that dynamical heterogeneity in glasses is directly correlated to the local structure. We also analyze the diffusion mechanisms of atoms in the liquid and glass states. It is found that for the mobile atoms in the glass state, initially they are confined in the cages formed by their nearest neighbors and vibrating. On the time scale of β relaxation, the mobile atoms try to break up the cage confinement and hop into new cages. In the supercooled liquid states, however, atoms continuously diffuse. Furthermore, it is found that on the time scale of β relaxation, some of the mobile atoms in the glass state cooperatively hop, which is facilitated by the stringlike cluster structures. On the longer time scale, it is found that a certain fraction of atoms can simultaneously hop, although they are not nearest neighbors. Further analysis shows that these hopping atoms form big and more compact clusters than the characterized most mobile atoms. The cooperative rearrangement of these big compact clusters might facilitate the simultaneous hopping of atoms in the glass states on the long time scale.

DOI: 10.1103/PhysRevB.77.184202 PACS number(s): 61.20.Ja, 61.43.Dq, 66.30.Fq

I. INTRODUCTION

Supercooled liquids and glasses are fascinating systems with complex structural and dynamical properties.[1] Our understanding of these systems is still far from complete. When a liquid is cooled far below its melting point, it exhibits a nonexponential relaxation behavior.[2] A number of experimental and molecular dynamics (MD) simulation studies have demonstrated that this nonexponential relaxation behavior can be attributed to the dynamical heterogeneity in the system.[3–22] For a supercooled liquid near the glass transition, dynamics in one region of the liquid can be orders of magnitude faster than that in another region. Kob *et al.*[8] studied the dynamical heterogeneities in a supercooled Lennard–Jones liquid using MD simulations. The mobile atoms in the supercooled liquid are identified and found to form clusters. Further computer simulations show stringlike cooperative atomic motion at temperatures well above the glass transition.[9,19,20] Below the glass transition, molecular dynamics simulation studies[17,21] using a binary Lennard–Jones mixture model suggested that dynamical heterogeneity may have a structural origin because the mobile atoms are surrounded by fewer neighbors.

The origin of dynamical heterogeneity in glass systems has been the focus of many recent studies.[23–32] The relationship between dynamical heterogeneities and local structures in supercooled liquid or glass systems has been investigated both theoretically and experimentally. Using MD simulations of equilibrium, glass-forming Lennard–Jones mixture, Donati *et al.*[19] characterized the local atomic motions and found that most atoms are trapped in cages and the motion of atoms is related to cage rearrangement. MD simulation for the dynamical heterogeneities below the glass transition suggested that dynamical heterogeneity may be due to the fact that mobile and/or immobile atoms are surrounded by fewer and/or more neighbors, which form an effectively wider and/or narrower cage.[17] In experiments of confocal microscopy, atom motion in colloidal systems was studied near the glass transition.[23] Cage rearrangements have been observed to involve localized clusters of atoms with large displacements, in regions with higher disorder and higher free volume.

Meanwhile, free-volume theory has been used to investigate the relation between the mobility of an atom and its local free volume.[24] MD simulations for a model supercooled polymer indicate a connection between the local free volume and dynamics.[25] A similar conclusion is also obtained from MD simulations in amorphous $Ni_{0.5}Zr_{0.5}$ below its glass temperature.[26] However, experiments on dense colloidal suspension with confocal microscopy and the corresponding computer simulations indicate a weak correlation between Voronoi volume and atom displacement.[27] Perera and Harrowell investigated the local structures and local relaxation times in two-dimensional glass-forming mixtures. They found no correlation at high temperatures and only weak correlation at low temperatures for the larger, less-mobile atoms.[28] In another approach, isoconfigurational ensemble was used to analyze dynamical and structural prop-

erties in simulations of a glass-forming molecular liquid.[11,29–31] Structural heterogeneities are found to correlate with dynamical heterogeneities. All of these previous studies indicate that the correlation between local structure and dynamical heterogeneities in supercooled liquid and glass is still an issue under intense debate.

Most of the previous studies have been performed on colloidal systems experimentally or Lennard–Jones systems computationally. In this paper, we perform MD simulations for the system of Al with a many-body interatomic potential based on the embedded atom method (EAM). While metallic glasses almost always occur in alloy systems, it is easier to start with a one-component system to understand the local structure and its relation with dynamics and diffusion processes. Our studies are based on recent EAM potential simulations,[33] which showed that it is possible to obtain both liquid and glass states at the same temperature for this EAM Al system.[33] In this paper, we will present results from analyses of the correlation between local structure and dynamical heterogeneity in this system using the supercooled liquid and glass structures generated in Ref. 33. In order to investigate the correlation between free volume and dynamics in the system, a local packing density is proposed to characterize the local environments of individual atoms. We also investigate the diffusion mechanisms in both supercooled liquid and glass states.

This paper is organized as follows: In Sec. II, a brief description of the model and simulation details is given. In Sec. III, we analyze the local structures in supercooled liquids and glasses. In Sec. IV, a local packing density is defined to investigate the local environment of each atom. The dynamics of atomic motion and its heterogeneity in liquids and glasses are examined in Sec. V. The correlation between dynamical heterogeneities and local structure is analyzed in Sec. VI. In Sec. VII, we examine the diffusion mechanisms in liquid and glass, and finally in Sec. VIII, discussion and conclusion are presented.

II. SIMULATION DETAILS

We perform molecular dynamics simulations of Al using the predict-correct algorithm with a time step of 0.5 fs. The EAM interatomic potential used in our calculations was developed by Ercolessi and Adams.[34] It can be expressed as

$$U_i = \frac{1}{2}\sum_{j(j\neq i)} \phi(r_{ij}) + \sum_i F(n_i). \quad (1)$$

Here, i and j denote distinct atoms, $\phi(r)$ is the pair interatomic potential, and $F(n)$ is the embedding energy function. Here, n_i is the total electron density at atom i due to all other atoms, and it is assumed that

$$n_i = \sum_{j(\neq i)} \rho(r_{ij}), \quad (2)$$

where $\rho(r_{ij})$ is the contribution to the electron density of atom i from a neighboring atom j. The values of the parameters of this potential were taken from Ref. 35.

In order to obtain the liquid,[33] we started with a random atomic configuration, and equilibrated it at $T=950$ K for 2 000 000 MD steps (the melting temperature of Al for this potential is about 925 K). The model consists of 2000 atoms in the simulation cell with periodic boundary conditions. The cell size was chosen to provide zero pressure in the NVT (i.e., $N=$const, $V=$const, and $T=$const) molecular dynamics simulation in which the system temperature is controlled by the velocity-adjustment method.

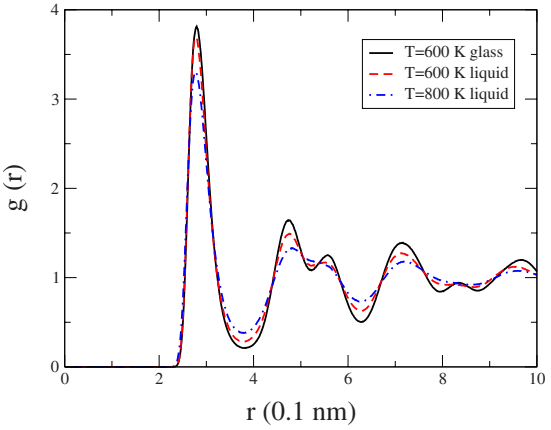

FIG. 1. (Color online) Pair correlation function of Al at various temperatures.

Next, we cooled down the liquid as follows: We decreased the temperature in steps of 50–100 K. After each step, the system was relaxed at constant temperature for 20 000 MD steps. The equilibrium density was determined by calculating the pressure for different cell volumes, and choosing the one whose pressure is close to zero. Then, we performed the MD simulation for the systems at the equilibrium density for another 20 000 MD steps.

For the glass state, we cooled the liquid model at $T=950$ K down to 300 K, keeping the pressure equal to zero, and relaxed it during 10 000 000 MD steps. Then, we heated up the glass state using the same procedure as described above for the liquid samples. The only difference was that the system required much longer time to equilibrate. In this way, we can get the structures of our systems in the supercooled liquid and glass states at various temperatures. More detailed information on the sample preparation can be obtained in Ref. 33. Our previous analysis[33] for all samples we obtained shows that all samples are properly equilibrated. In this paper, we analyze the behavior of the system in the supercooled liquid state at 600 and 800 K and in the glass state at 600 K. Their volumes are 32.496 94, 32.726 68, and 33.13791 Å, respectively. Atomic coordinates are collected over an interval of 2 000 000 MD steps for structural and dynamical analyses of these systems.

III. ANALYSIS OF THE LOCAL STRUCTURE IN SUPERCOOLED LIQUID AND GLASS OF Al

Figure 1 shows the pair correlation functions for the supercooled liquids at 600 and 800 K and glass at 600 K, respectively. The height of the first peak increases when the liquid is cooled down from 800 to 600 K, which indicates that the atomic ordering in the first coordination shell in-

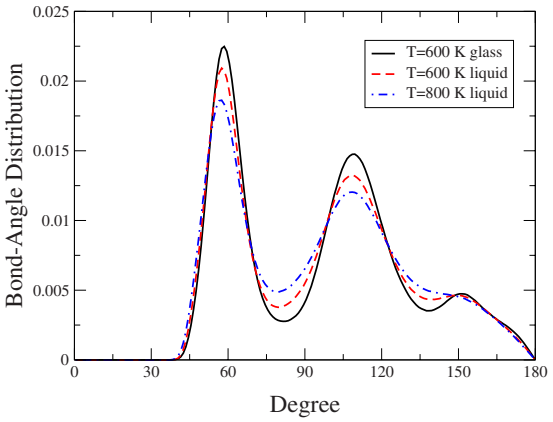

FIG. 2. (Color online) Bond-angle distribution of Al at various temperatures.

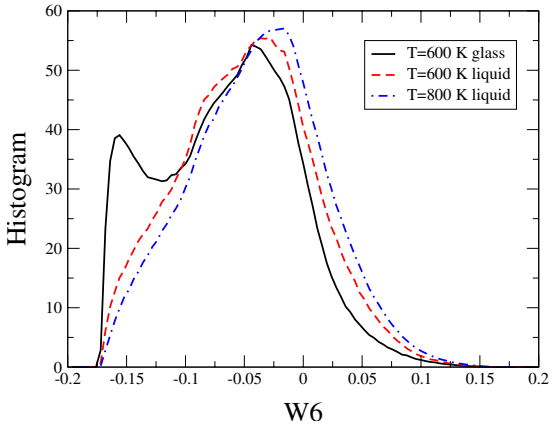

FIG. 3. (Color online) Histogram of W_6 in glass and supercooled liquid of Al at $T=600$ and 800 K.

creases as temperature decreases. The atomic ordering in the first coordination shell of the glass state is slightly better than that in the supercooled liquid state although the temperatures of the two states are both 600 K. Overall, the pair correlation functions only display minor differences between the supercooled liquid and glass states.

A more comprehensive picture of the short-range order in a liquid requires knowledge not only of the number and length of the bonds, but also of their directions. Here, we investigate the bond-angle distributions for those samples, as shown in Fig. 2. The typical shape of the distribution contains a distinct peak around 60° associated with equilateral-triangular configurations and a second broad hump at around 110°. The number of nearly equilateral triangles increases as temperature decreases in the undercooling regime and below the glass transition. There is a third peak around 150°, which is very pronounced in the glass state and smeared out in the liquid state when the temperature is increased. Therefore, this peak at 150° may be related to the structure features in the glass state.

It is generally believed that supercooled liquids and glasses lack the long-range translational periodic order of a crystalline solid, but exhibit a significant amount of short-range order. The possible existence of local icosahedral fivefold symmetry was proposed by Frank.[36] The concept of icosahedral short-range order (ISRO) has been confirmed by several molecular dynamic computer simulations based on empirical potentials.[37–40] Recently, experimental evidence for the presence of fivefold symmetry was obtained in liquid Pb.[41] Neutron scattering experiments also suggest ISRO in undercooled elemental metallic melts.[42,43] In addition, ISRO in amorphous solids was observed using local environment probes.[44,45] Experimental data also show a correlation between nucleation barriers and growing ISRO with decreasing temperature in metallic liquids.[46] In order to obtain a deeper insight into possible ISRO in our liquid and glass structures, we perform a detailed analysis of our system geometries with a set of bond orientation order parameters introduced by Steinhardt *et al.*[37]

The most sensitive indicator for icosahedral symmetry is the W_6 parameter, which is calculated using averages of spherical harmonics associated with the bond directions.[37] For example, for the center atom in an isolated 13-atom cluster with an icosahedral, fcc, or hcp symmetry, the W_6 value will be −0.1698, −0.013 16, and −0.0124 42, respectively.[37]

Figure 3 shows the histogram of W_6 in different supercooled liquid and glass samples. As one can see in Fig. 3, the W_6 distribution is found to be very broad and strongly asymmetric, spreading from negative values close to −0.17 to positive values bigger than 0.1. For the liquid at 800 K, the distribution of the W_6 has a main peak at the value a little bit below zero and also exhibits a modest shoulder around the value of −0.15, as can be seen in Fig. 3. As temperature decreases to 600 K, the peak shifts to the left, and the population of the local structures close to icosahedron slightly increases. In the glass state at $T=600$ K, as shown in Fig. 3, an additional peak appears around −0.17, which indicates the presence of icosahedral structure in a substantial fraction of the system. ISRO is much stronger in the glass state than in the liquid states.

IV. LOCAL ENVIRONMENT: LOCAL PACKING DENSITY OF INDIVIDUAL ATOMS

As mentioned in Sec. I, Voronoi tessellation is a common tool to measure the local free volume of each atom in disordered systems. The connection between local free volume and mobility of atoms in liquid and glass systems has been the subject of several studies, but at present there is still no clear consensus on this issue.[25–28] Here, we introduce a concept, local packing density, to describe the local environment of liquid and glass. The local packing density of an atom i can be defined as a summation of the contributions for each of its neighbors j through a Gaussian distribution. That is,

$$\rho_i = \left(\frac{\alpha}{2\pi}\right)^{3/2} \sum_j \exp[-\alpha(\mathbf{r}_i - \mathbf{r}_j)^2]. \tag{3}$$

Here, j runs over all atoms within a cutoff distance (which is chosen to be 10 Å in our calculations) from atom i. α describes the width of the Gaussian function, which is chosen so that the local environment of individual atom in liquid and glass is optimally distinguishable by the local packing density. If α is too big, the packing density distribution of a

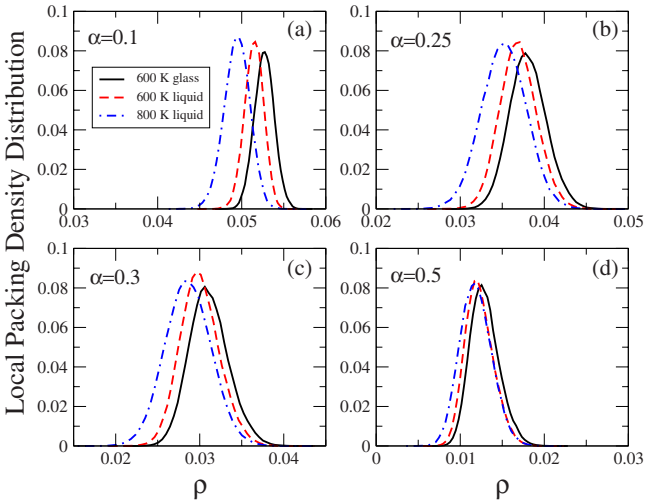

FIG. 4. (Color online) Local packing density distributions in supercooled liquid and glass states of Al for different values of α.

liquid or glass sample will be very narrow and sharp, because each atom in the sample hardly feels the presence of its neighbors. On the other hand, if α is too small, the packing density distribution is also narrow and sharp because the information from the neighboring atoms is smeared out and the local environment becomes indistinguishable. The optimal choice of α will make the distribution of local packing density in a given liquid or glass sample as broad as possible. In order to find an optimal value for α, we calculated the packing density distributions with various values of α for the three liquid and glass samples discussed in this paper. As shown in Fig. 4, for a small and a big α of 0.1 and 0.5, the local packing density distributions in all three samples are quite narrow, as shown in Figs. 4(a) and 4(d). For $\alpha \approx 0.25$ or 0.3, however, the packing density distributions are quite broad for all three samples, as shown in Figs. 4(b) and 4(c).

For a liquid state, the packing densities of atoms are relatively small and the distribution is relatively broad. On the contrary, for a glass state, the local packing densities of atoms are relatively bigger and the distribution is narrower. This behavior is reasonable. Thus, we can use the local packing density defined above as a measure of the local environment of each atom in liquid and glass states. In order to obtain the best value of α, we calculated the half-width of the packing density distribution for each sample, as shown in Fig. 5, and $\alpha=0.25$ is used in the calculations of local packing density in the rest of the paper.

V. DYNAMICAL HETEROGENEITY: MOBILE AND IMMOBILE ATOMS

We investigated the dynamics and its heterogeneity in the liquid and glass states of Al from our simulation in order to gain some understanding of how the local structure affects the dynamics of atoms in liquid and glass states. First, we investigate the evolution of mean square displacements (MSDs) of atoms with time for each sample. Figure 6 shows the typical behavior of MSD vs time t in supercooled and amorphous states.[47] On the short time scale, all curves show

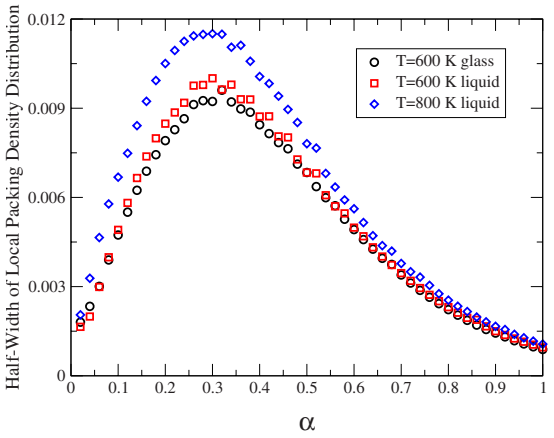

FIG. 5. (Color online) Variation of half-width of the local packing density distributions with α for supercooled liquid and glass states of Al.

a power-law behavior, which indicates that the motion of atoms is ballistic. For the amorphous state of Al at $T=600$ K, after the power-law behavior the curve shows a plateau, which indicates that the diffusivity in the glass is quite small during this period of time after the ballistic motion. On this time scale, atoms are confined in the cages formed by their nearest neighbor atoms. On the long time scale, the curve shows power-law behavior again, which means the atoms break up the confinement, and the motion of atoms go into a diffusive regime. For the supercooled liquid at $T=600$ K, the plateau can still be seen but it does not last as long as it is in the glass state of $T=600$ K. For the supercooled liquid at 800 K, the plateau is hardly seen. The motion of atoms almost go from ballistic directly into diffusive, since this temperature is close to the melting point. This plot clearly shows that the dynamics of the system at different temperatures or states is quite different. The atoms in liquids are much more mobile than those in glass states. The mobility of atoms increases with temperatures. Figure 6 also indicates that all samples in our simulation are in the equilibrium states.

In order to investigate the dynamical heterogeneity in this system, we examine the time dependence of the self-part of

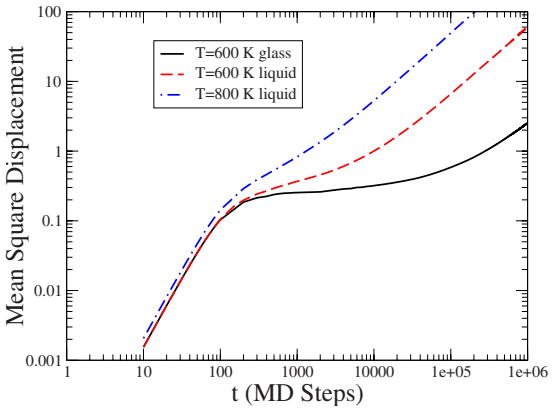

FIG. 6. (Color online) Mean square displacement in supercooled liquids and glasses of Al at 600 and 800 K.

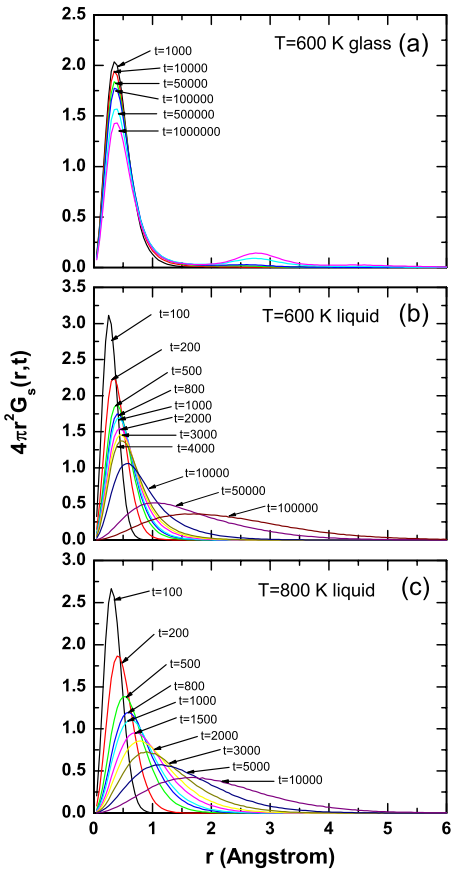

FIG. 7. (Color online) $4\pi r^2 G_s(r,t)$ versus r at various times t. (a) $T=600$ K in the glass state, and (b) $T=600$ K and (c) $T=800$ K in supercooled liquid states, respectively.

the Van Hove correlation function,[47,48] $G_s(r,t)$, where r is the distance traveled by an atom in a time t. Previous studies showed that it has a Gaussian form, but deviates from the form at intermediate times, indicating the presence of dynamical heterogeneity.[49] Figure 7 shows $4\pi r^2 G_s(r,t)$ at $T=600$ K in the glass state, and $T=600$ K and $T=800$ K in supercooled liquid states, respectively. As discussed in our previous analysis,[33] Fig. 7(a) shows that in the glass state of 600 K, most atoms do not diffuse but rather vibrate near their equilibrium positions. In the supercooled liquid states, however, atoms diffuse to larger distance with time. Interestingly, there is a second peak in the distribution in the glass state as shown in Fig. 7(a), which indicates that there is a preferable diffusion jump distance in the glass state of Al at $T=600$ K. This issue will be discussed in more detail later.

We also investigate the non-Gaussian parameter,[50]

$$\alpha_2(t) = \frac{3\langle r^4(t)\rangle}{5\langle r^2(t)\rangle^2} - 1, \tag{4}$$

which characterizes the deviations of $G_s(r,t)$ from a Gaussian form. Figure 8 shows $\alpha_2(t)$ as a function of t for the glass at $T=600$ K, and the supercooled liquid at $T=600$ K and $T=800$ K, respectively. The behavior is similar to that found in the previous studies.[8,47] On the short time scale of ballistic motion of atoms, α_2 is zero. As the system enters the time

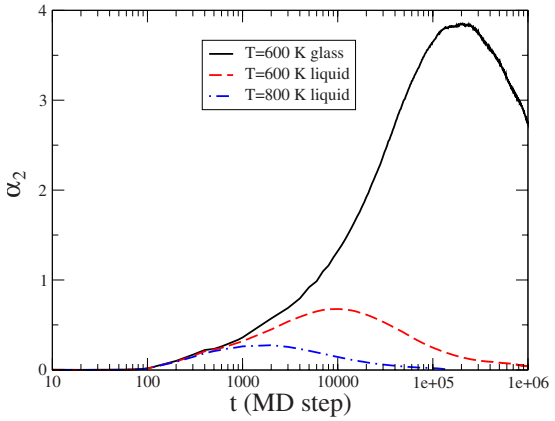

FIG. 8. (Color online) Non-Gaussian parameter α_2 versus time t for $T=600$ K in the glass state, and $T=600$ K and $T=800$ K in supercooled liquid states, respectively. t^* denotes the time at which α_2 reaches the maximum.

scale of the β relaxation, α_2 begins to increase. It reaches the maximum around the end of the β relaxation region. On the time scale of α relaxation, it decreases to zero. As temperature decreases, the position of the maximum t^* shifts toward longer times, and the value of α_2 also increases. This indicates that the dynamical heterogeneity is getting stronger as temperature decreases, and much stronger in glass state than in liquid states.

Most studies on the dynamical heterogeneity in supercooled liquid and glass tried to monitor a certain percentage of the fastest ("mobile") or slowest ("immobile") atoms, and analyzed their spatial distributions. Here, we adopt the same approach. We characterize the mobility of each atom by calculating the mean square displacement in the time interval defined by t^*, since t^* is the time at which the distribution of atom displacements has the largest deviation from the Gaussian distribution, and may also be the moment when the liquid is likely to be most dynamically heterogeneous.[8] We select 100 atoms (5% of all atoms) with the largest mean square displacements as the mobile (fastest) atoms. In the same way, we identify 100 atoms with the smallest mean square displacements as the immobile (slowest) atoms.

Figure 9 shows the snapshots of mobile and immobile atoms in the supercooled liquid and glass at $T=600$ K. In the glass state, it can be seen that both mobile and immobile atoms tend to form clusters, and the distributions are not uniform, as shown in Figs. 9(a) and 9(b). This demonstrates that the dynamics of atoms in the glass state is heterogeneous. Comparing Figs. 9(a) and 9(b), it is clear that mobile and immobile atoms tend to segregate. In some regions, atoms are relatively active. In some other regions, atoms are not. In supercooled liquids at $T=600$ K, however, such a trend of clustering is not as obvious as in the glass. As we can see in Figs. 9(c) and 9(d), the distributions in supercooled liquids are relatively broad and random. We also checked the distributions of mobile and immobile atoms in other liquid samples at higher temperatures. As temperature approaches the melting point, the distributions of mobile and immobile atoms in the corresponding sample are even more random. Therefore, as temperature decreases, the dynamics

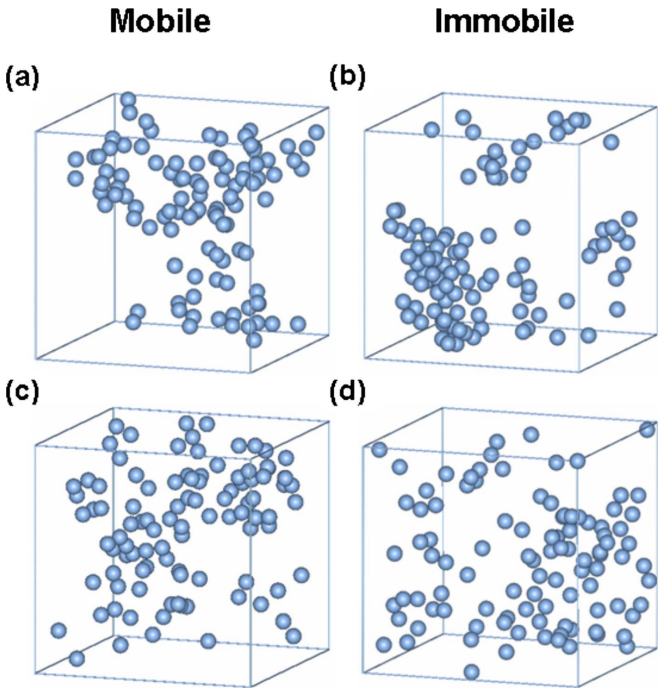

FIG. 9. (Color online) Snapshot of the positions of mobile and immobile atoms in supercooled liquid and glass of Al at $T=600$ K at time t^*. (a) Mobile atoms in glass, (b) immobile atoms in glass, (c) mobile atoms in liquid, and (d) immobile atoms in liquid.

of atoms in the system is getting more heterogeneous as the system slows down.

We notice that in the glass state, the clusters formed by immobile atoms are more compact than those formed by mobile atoms, which can be seen clearly in Figs. 9(a) and 9(b). However, the mobile atoms tend to form stringlike clusters, consistent with the picture proposed by Donati *et al.*[9,19]

The analysis of the spatial correlation between mobile atoms $[g_{MM}(\mathbf{r})]$, immobile atoms $[g_{II}(\mathbf{r})]$, and also between mobile and immobile atoms $[g_{MI}(\mathbf{r})]$ will be very useful to examine the spatial distributions of the mobile and immobile atoms. Here, I and M represent the immobile and mobile atoms, respectively. $g_{MI}(\mathbf{r})$ is defined as[19]

$$g_{MI}(\mathbf{r}) = \frac{V}{N_I N_M} \sum_{\substack{i=1 \\ i\in N_I}}^{N_I} \sum_{\substack{j=1 \\ j\in N_M}}^{N_M} \delta(\mathbf{r} + \mathbf{r}_j - \mathbf{r}_i) \tag{5}$$

and $g_{MM}(\mathbf{r})$ or $g_{II}(\mathbf{r})$ is defined as

$$g_{aa}(\mathbf{r}) = \frac{V}{N_a(N_a-1)} \sum_{\substack{i=1 \\ i\in N_a}}^{N_a} \sum_{\substack{j=1, j\neq i \\ j\in N_a}}^{N_a} \delta(\mathbf{r} + \mathbf{r}_j - \mathbf{r}_i). \tag{6}$$

Here, a denotes I and M. $N_I=N_M=100$ are the number of immobile and mobile atoms, respectively. V is the volume of the system. Assuming rotational invariance, the correlation functions do not depend on the direction of $\mathbf{r}$, but only on the distance $r=|\mathbf{r}|$, so we calculate $g_{MM}(r)$, $g_{II}(r)$, and $g_{MI}(r)$.

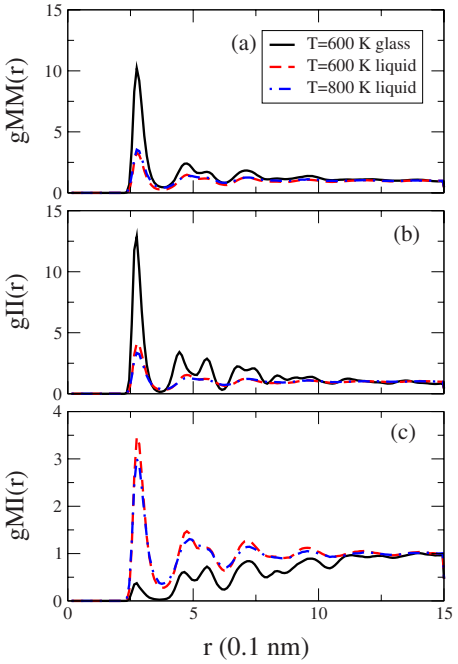

FIG. 10. (Color online) Pair correlation functions $g_{MM}(r)$ (a), $g_{II}(r)$ (b), and $g_{MI}(r)$ (c) for the mobile and immobile atoms in supercooled liquid and glass of Al at $T=600$ and 800 K, respectively.

Figure 10 shows the pair correlation functions $g_{MM}(r)$ between mobile atoms, $g_{II}(r)$ between immobile atoms, and $g_{MI}(r)$ between mobile and immobile atoms in glass and supercooled liquid states, respectively. It is found that in the glass state, the mobile (immobile) atoms are strongly correlated at short and intermediate distances. This indicates that mobile (immobile) atoms tend to stay together and form clusters. The pair correlation between mobile and immobile atoms in the glass state is suppressed at short distances. In the glass state, atoms in some regions are relatively active and mobile, but atoms in some other regions are not so dynamic. The active regions and inactive regions do not overlap.

In contrast, in supercooled liquids, the pair correlation functions for the mobile, immobile, mobile vs immobile atoms are similar, which probably indicates that atoms alternate between mobile and immobile behaviors during the simulation time scale, so that there is no major difference between mobile and immobile atoms.

VI. CORRELATION BETWEEN LOCAL STRUCTURE AND DYNAMICS IN SUPERCOOLED LIQUID AND GLASS OF Al

In this section, we will address the issue whether there is a correlation between local structure or local environment and dynamical heterogeneity. As we discussed in Sec. I, although there have been a lot of work done by computer simulations and experiments, the answer to this question is still not clear.

We perform our analysis along two approaches. In the first approach, we select the instantaneous atomic configura-

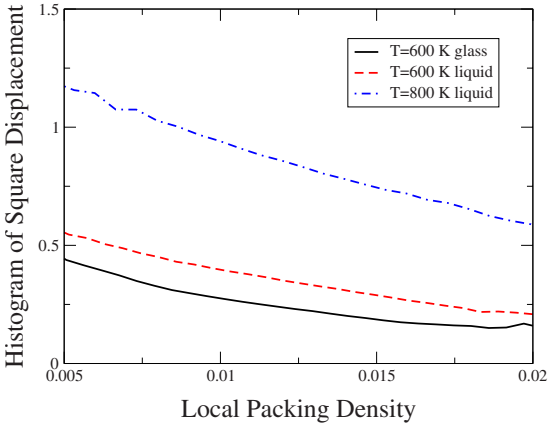

FIG. 11. (Color online) Correlation between square displacements of atoms in 1000 MD step time interval and local packing density in supercooled liquid and glass states of Al. Snapshot configurations are used.

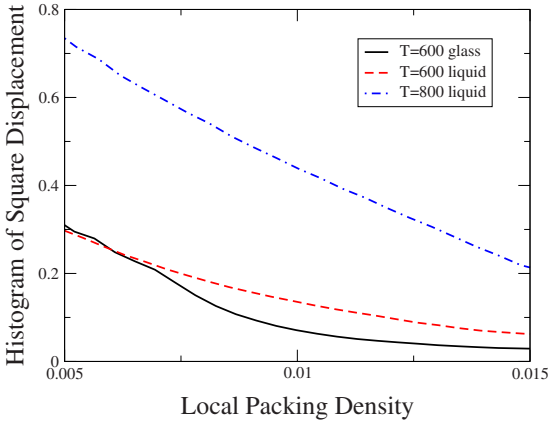

FIG. 12. (Color online) Correlation between square displacements of atoms in 1000 MD step time interval and local packing density in supercooled liquid and glass states of Al. Averaged configurations are used.

tion every 1000 MD steps from the 2 000 000 MD steps of simulations of the supercooled liquid or glass. The square displacement of each atom between successive snapshots and the local packing density of the atom are calculated for each snapshot. For the local packing density, we divide them into several regions from the lowest to the highest. Then, we sort all of the atoms in the selected 2000 snapshot configurations with their local packing densities, and average the square displacements of those atoms with similar local packing density. Finally, the statistics of the correlation between the local packing density and square displacement are analyzed over all the atoms in 2000 snapshot configurations.

In the second approach, the atomic coordinates are averaged over every 1000 MD steps in order to minimize the noise due to thermal vibration. The local packing density for each atom is calculated using the "averaged" atomic coordinates. The square displacement of each atom in the 1000 MD step time interval is also calculated using the same averaged atomic coordinates. In the same way used in the first approach, we analyze the statistics of the correlation between the local packing density and square displacement over 2000 averaged configurations, which are obtained from the 2 000 000 MD simulation steps.

Figures 11 and 12 show the correlation between square displacement of atoms and local packing density obtained from the above two types of analyses, respectively. We shift the minimum value of the local packing density of each sample to zero, so we can make an easy comparison. We also remove the two ends (i.e., low and high local packing density ends) of these curves in Figs. 11 and 12 because of the poor statistics at these two extremes. As shown in Figs. 11 and 12, it is clear that in both glass and liquid states, the dynamics of atoms strongly correlate with their local packing densities. The atoms with lower packing densities on the average travel farther than those with higher packing densities in the same time interval. Therefore, in the regions where local packing densities of atoms are higher, atoms are in general less mobile; while in the regions where local packing densities of atoms are lower, atoms are more mobile.

The behavior of the correlation between the mobility and the local packing density of atoms in supercooled liquid and glass states is similar to that of mean free path and number density of gases predicted by kinetic theory of gases.[51] The mean free path of gases is in inverse proportion to the number density of gases. If the number density is higher (lower), the mean free path will be smaller (larger). In this sense, there should exist a correlation between the mobility and local density of atoms in supercooled liquid and glass states.

We also investigate the local packing density distribution of mobile and immobile atoms in liquid and glass states, respectively. The averaged configuration of every 1000 MD steps is used to calculate the local packing density of each atom. Figure 13 shows the local packing density distributions for total atoms, mobile and immobile atoms at 600 K in the liquid and glass states, respectively. In the glass state the local packing density distribution of the mobile atoms is

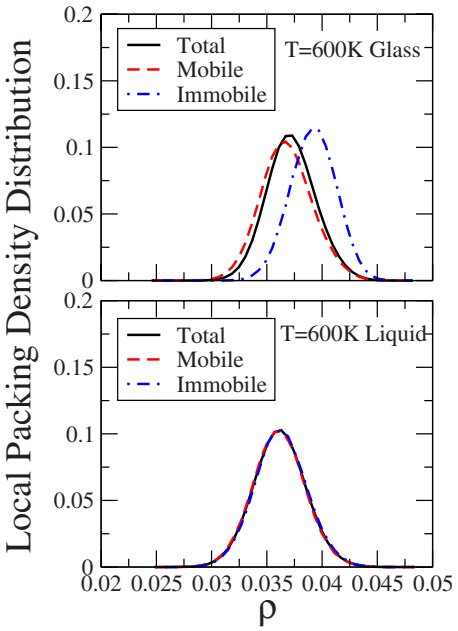

FIG. 13. (Color online) The local packing density distributions for total atoms, mobile, and immobile atoms at $T=600$ K in liquid and glass states, respectively.

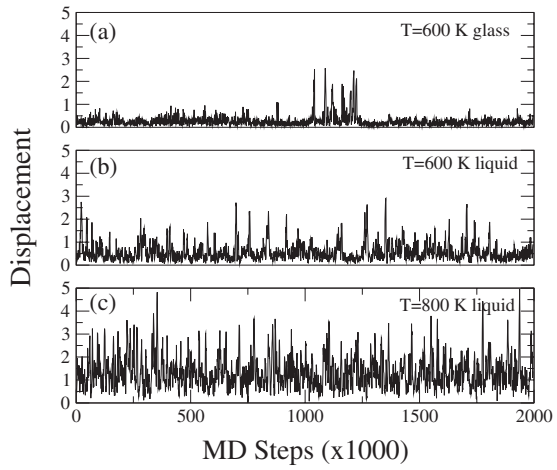

FIG. 14. The displacement of a mobile atom between each 5000 MD steps in supercooled liquids and glasses of Al at $T=600$ K and $T=800$ K, respectively.

quite different from that of the immobile atoms. As we mentioned above, mobile atoms have bigger free volumes than immobile atoms. In the liquid state, the local packing density distributions are the same for all types of atoms. This indicates that in the liquid state, the correlation between the mobility and local packing density could be smeared out if their averaged values over long simulation time are used for the correlation analysis.

VII. DIFFUSION MECHANISMS IN SUPERCOOLED LIQUIDS AND GLASS STATES OF Al

Diffusion mechanisms in supercooled liquid and glass have been a subject of intensive studies. Computer simulations of a hard sphere system close to the glass transition by Doliwa and Heuer[52] have shown a cage effect on the single-atom dynamics: Individual atoms are trapped in the cages formed by their neighbors, vibrating in the cages, and then leaving the cages quickly. The motion of atoms is essentially a hopping process. Diffusion mechanisms in Zr-based metallic supercooled liquids and glasses were also studied by experiment using nuclear magnetic resonance.[53] Two distinct processes, single-atom hopping and collective motion, are identified in the supercooled liquid state, but the latter is the dominant process. Furthermore, experimental measurements of the mass dependence of Co diffusion in Co_xZr_{1-x} glasses and in both glassy and supercooled liquid states of a $Pd_{40}Cu_{30}Ni_{10}P_{20}$ system suggested that diffusion of atoms occurs via highly collective hopping processes.[54,55] Cooperative motion of atoms in the supercooled liquid state was also suggested in MD simulations.[9,20,56] In this section, we will investigate the diffusion mechanisms of atoms in both supercooled liquid and glass states of Al.

Figure 14 shows the time variation of displacement of a typical mobile atom in every 5000 MD steps in the supercooled liquid and glass states, respectively. The displacement presented in this figure is defined as the displacement of an atom with respect to its previous (not the original) position at every 5000 MD steps. The motion behavior of atoms in the glass state is quite different from that in the liquid state. As shown in Fig. 14(a), at most times the displacements of atoms in the glass state are very small. The atoms can only vibrate in small regions enclosed by their nearest neighbors. Occasionally, some atoms jump out of their original positions to new ones, then are trapped in other small regions and keep vibrating again. For some immobile atoms, they might never leave their original positions in the whole simulations. This motion mechanism indicates the cage effect on the atoms as mentioned above.

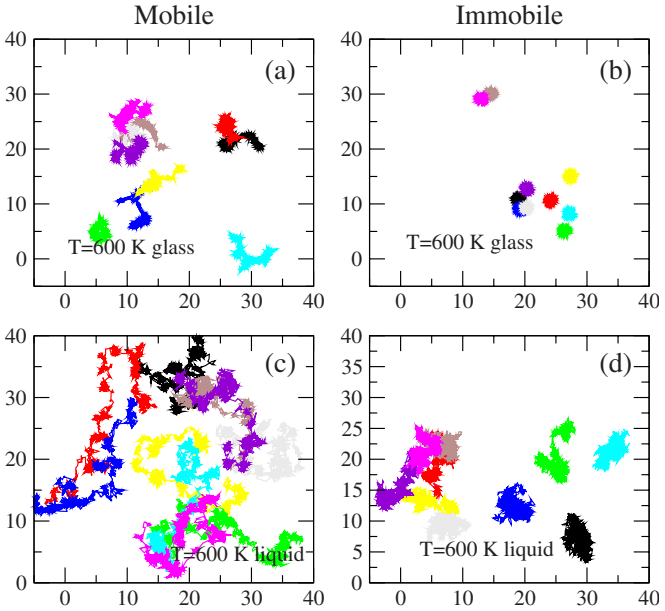

FIG. 15. (Color online) Trajectories projected on the XY plane of the ten mobile [(a) and (c)] and ten immobile atoms [(b) and (d)] in supercooled liquid [(c) and (d)] and glass [(a) and (b)] of Al at $T=600$ K. In each panel, different colors represent different atoms.

In contrast, atoms in the liquid are more active, they keep on moving from one position to another during the simulation, as shown in Figs. 14(b) and 14(c). While the cage effect also affects the motions of atoms in liquid states, they can easily escape the cage confinement and leave. Therefore, atoms in the liquid move more continuously. In the glass state, atoms are trapped in cages most of the time, and only escape occasionally. Such diffusion mechanisms have been demonstrated by the self-part of the Van Hove correlation function, as shown in Fig. 7. The second peak shown in Fig. 7(a) indicates a preferable hopping distance in the glass state of Al at $T=600$ K. This behavior is similar to that observed in the two-component amorphous Lennard–Jones system.[11] It results from rare jumps of atoms over the distance roughly equal to the interparticle separation.

We monitored the trajectories of some mobile and immobile atoms over the simulations. Figure 15 shows the trajectories over 2 000 000 MD steps projected onto the XY plane for some mobile and immobile atoms in the liquid and glass at 600 K, respectively. The diffusion mechanisms in liquid and glass states are quite different. In the glass state, immobile atoms are locally vibrating, and never leave their original positions. Mobile atoms succeed in escaping confinement. Some of them jump multiple times, far away from

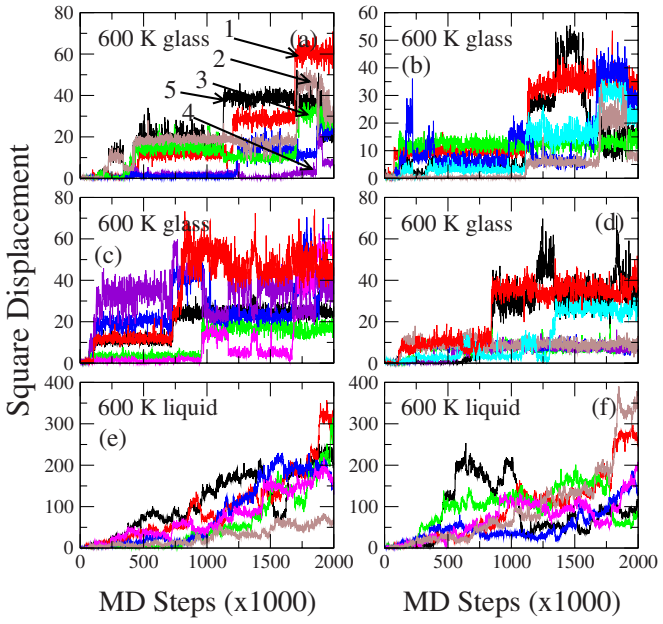

FIG. 16. (Color online) Square displacements of a mobile atom and some of its initial nearest neighbor atoms who can hop during simulations in glass [(a)–(d)] and supercooled liquid [(e) and (f)] of Al at $T=600$ K, respectively. In each panel, different colors represent different atoms. Black represents the selected atom, and other colors represent some initial nearest neighbors of this selected atom. In (a), 1, 2, 3, 4, and 5 denote the curves of the square displacement for different five atoms.

their original positions. For the atoms in supercooled liquid of $T=600$ K, the situation is quite different, as shown in Figs. 15(c) and 15(d). Even immobile atoms are much more active than the mobile atoms in the glass state. The trajectories of atoms in the supercooled liquids are more continuous.

Whether do the atoms in glass states hop individually or cooperatively? This issue is important because it is correlated to the dynamical relaxation in a supercooled liquid or amorphous system. If atoms move cooperatively, they are most likely the nearest neighbors. Therefore, we will examine the diffusion processes of the mobile atoms and their nearest-neighbor atoms. For the mobile atoms, as we discussed above, initially they are confined in the cages formed by their nearest neighbors. On the time scale of β relaxation, these mobile atoms break up the confinement of the cages, and hop into new cages. As found in previous studies, some mobile atoms hop cooperatively, and such a cooperative motion of mobile atoms is facilitated by the stringlike clusters.[4–9]

Figure 16 shows the square displacements of mobile atoms (with respect to their initial positions) and some of their initial nearest neighbors with time in the supercooled liquid and glass states, respectively. Each panel represents one mobile atom and some of its initial nearest neighbors. For the glass state of $T=600$ K, only the nearest neighbors who can hop away from the original positions are considered. For the liquid state of $T=600$ K, all nearest-neighbor atoms can move away from their initial positions, so only some of them are presented here. In the supercooled liquid, the motion of atoms is relatively continuous, and the diffusion of atoms is not correlated in time, as shown in Figs. 16(e) and 16(f). All atoms diffuse together, but some diffuse faster and some diffuse slower. This motion is more like liquid flowing.

However, as shown in Figs. 16(a)–16(d), in the glass state the hopping of neighboring atoms is correlated in time, indicating cooperative motion during the diffusion process. Some atoms move together for a while, then decouple at some point of time, as shown in Fig. 16(d), as they move away from each other. After that, they might move individually, or move together with some other atoms.

In Figs. 16(a)–16(d), we notice that in the glass state atoms are hopping at almost the same time even when they are not nearest neighbors. For a mobile atom and some of its nearest neighbors, for example in Fig. 16(a), atom 5 is the selected mobile atom, and atoms 1–4 are the nearest neighbor atoms of it. However, atoms 1–4 might not be the nearest neighbors to each other. Initially, they are vibrating together. At around the 200 000th MD step, atom 2 hops away from its original position with atom 5. Atoms 1, 3, and 4 are still in their original positions. At around the 400 000th MD step, atoms 1 and 3 hop together away from their original positions. At the same time, atoms 2 and 5 are hopping, too. They might or might not be the nearest neighbors, but atom 4 is not because it is still in its original position. At the time around the 1 700 000th MD step, atoms 1, 2, and 3 hop almost simultaneously into respective new regions. At this time, all five atoms might not be the nearest neighbors anymore. At the time around the 1 900 000th MD step, however, these five atoms still hop at the same time. This simultaneous hopping of atoms can also be seen in the motion of other atoms, as shown in Figs. 16(b)–16(d). This demonstrates a cooperative motion of atoms in the glass state. Therefore, the mobile atoms together with some of their nearest neighbors move in a cooperative way in the glass states. Most of the time, they just vibrate. They simultaneously hop sometimes even when they are not the nearest neighbors.

As mentioned in the above sections, in the β relaxation regime, mobile atoms tend to form stringlike clusters, which facilitate the cooperative motion of some mobile atoms.[9,20] For the simultaneous hopping of atoms shown in Figs. 16(a)–16(d), it might be also facilitated by the stringlike structures. Here, we will investigate the spatial distributions of these hopping atoms. First, we identify the first 20 most mobile atoms and their nearest neighbors, which can hop at least once in the time scale of the simulations. As a result, the number of such atoms are about 120. Then, we monitor the positions of the selected atoms at different times, as shown in Fig. 17. Figure 17 shows the snapshot of the positions of these atoms at (a) $t=0$, (b) $t=1\,000\,000$ MD steps, and (c) $t=2\,000\,000$ MD steps, respectively. It is clearly shown that these hopping atoms form very compact clusters. Initially, they form roughly four compact clusters with different sizes, three bigger and one smaller. With time increasing, these clusters become less dense, and tend to connect with each other.

We notice that these clusters formed by these hopping atoms are bigger and much more compact than those formed by the mobile atoms defined in the time interval of t^*, as shown in Fig. 9(a). Therefore, the simultaneous hopping of atoms observed in our simulations might not be correlated to the stringlike structures, but the relatively compact onces.

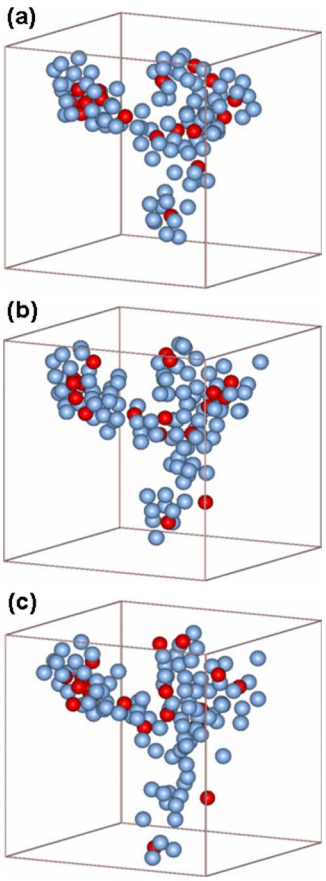

FIG. 17. (Color online) Snapshot of the positions of the atoms, which can hop in the time scale of our simulations in the glass state of $T=600$ K at (a) $t=0$, (b) $t=1000\,000$ MD steps, and (c) $t=2000\,000$ MD steps, respectively. The dark and light balls represent the mobile atoms and their initial nearest neighbors, which can hop in the simulations.

However, why are the atoms in these rather compact clusters able to hop, even simultaneously at some times on the longer time scale? A similar behavior was also observed in the democratic particle motion metabasin transitions in α relaxation in a simple Lennard–Jones glass-forming system.[56] It was found that the metabasin transitions involve the collective motion of around 30–60 particles that form a relatively compact cluster. Such a cooperative rearrangement of a substantial fraction of the particles is responsible for the α relaxation.[56] In our case, the hopping atoms form compact clusters. The cluster size is in the range of 30–60 atoms. Therefore, it could be the cooperative rearrangement of the atoms in the compact clusters that facilitates the simultanous hopping on the long time scale observed in our simulations. Our findings are consistent with the picture of cooperatively rearranging regions proposed a long time ago.[57]

VIII. DISCUSSION AND CONCLUSION

We have analyzed the local structure, local environment, and dynamical heterogeneity in supercooled liquid and glass states of Al through molecular dynamics simulation using an empirical interatomic potential. As shown above, the pair correlation functions and bond-angle distributions of the supercooled liquid and glass samples display only small differences. However, the ISRO, i.e., frequency histogram of W_6, is quite different. In liquid state, the population of atoms with ISRO is small, while the population of atoms with ISRO in the glass state significantly increases. We also found that the ISRO allows a denser packing of atoms locally.

The dynamics analysis in liquid and glass states of Al shows that mobile (immobile) atoms tend to form clusters in the glass state. However, in the liquid, cluster formation is not as obvious. Furthermore, the clusters formed by immobile atoms are more compact than those formed by mobile atoms. As observed in some previous studies, mobile atoms form stringlike clusters, which make the atoms diffuse more easily. The partial correlation function analysis also shows that the spatial correlation between mobile and immobile atoms in the glass state is stronger than that in the liquid state. Mobile and immobile atoms have a tendency to segregate. All of these indicate dynamical heterogeneous behavior in the glass state.

We also investigate the local environment of individual atoms by a definition of local packing density. More detailed analysis shows that there is a connection between local structures or environments and dynamical heterogeneity in both liquid and glass states. In the regions where local packing densities are lower, the atoms are more mobile.

Atoms in the liquid are more active than in the glass. In the glass state, atoms diffuse mainly by hopping. Moreover, the mobile atoms in the glass collectively diffuse. On the longer time scale, mobile atoms and some of other atoms hop almost simultaneously sometimes, even when they are not nearest neighbors. Some hop over a relatively long distance, but others only hop a very short distance. It is found that on the long time scale, these atoms who can hop form relatively compact clusters. These compact clusters rearrange with time and facilitate the cooperative hopping. Therefore, the cooperative hopping of atoms should be the main diffusion mechanism in the glass state. It is also found that in the glass state, the dyanmical relaxation of the system on the long time scale might involve a cooperative rearrangement of a fraction of atoms that form relatively compact clusters. In the liquid, atoms continuously diffuse.

ACKNOWLEDGMENTS

The work at Ames Laboratory was supported by the U.S. Department of Energy, Basic Energy Sciences, including a grant of computer time at the National Energy Research Supercomputing Center (NERSC) in Berkeley, under Contract No. DE-AC02-07CH11358. M.L. was also supported by the Startup Grant of Renmin University of China. We thank Jörg Schmalian for valuable discussion.

[1] M. D. Ediger, C. A. Angell, and S. R. Nagel, J. Phys. Chem. **100**, 13200 (1996); P. G. Debenedetti and F. H. Stillinger, Nature (London) **410**, 259 (2001).
[2] R. Richert, J. Non-Cryst. Solids **209**, 172 (1994).
[3] S. C. Glotzer and C. Donati, J. Phys.: Condens. Matter **11**, A285 (1999).
[4] M. D. Ediger, Annu. Rev. Phys. Chem. **51**, 99 (2000).
[5] S. C. Glotzer, J. Non-Cryst. Solids **274**, 342 (2000).
[6] R. Richert, J. Phys.: Condens. Matter **14**, R703 (2002).
[7] H. C. Andersen, Proc. Natl. Acad. Sci. U.S.A. **102**, 6686 (2005).
[8] W. Kob, C. Donati, S. J. Plimpton, P. H. Poole, and S. C. Glotzer, Phys. Rev. Lett. **79**, 2827 (1997).
[9] C. Donati, J. F. Douglas, W. Kob, S. J. Plimpton, P. H. Poole, and S. C. Glotzer, Phys. Rev. Lett. **80**, 2338 (1998).
[10] R. Yamamoto and A. Onuki, Phys. Rev. Lett. **81**, 4915 (1998).
[11] S. Sastry, P. G. Debenedetti, and F. H. Stillinger, Nature (London) **393**, 554 (1998).
[12] W. K. Kegel and A. van Blaaderen, Science **287**, 290 (2000).
[13] E. R. Weeks, J. C. Crocker, A. C. Levitt, A. Schofield, and D. A. Weitz, Science **287**, 627 (2000).
[14] D. Caprion, J. Matsui, and H. R. Schober, Phys. Rev. Lett. **85**, 4293 (2000).
[15] C. Kaur and S. P. Das, Phys. Rev. Lett. **86**, 2062 (2001); **89**, 085701 (2002).
[16] X. Xia and P. G. Wolynes, Phys. Rev. Lett. **86**, 5526 (2001).
[17] K. Vollmayr-Lee, W. Kob, K. Binder, and A. Zippelius, J. Chem. Phys. **116**, 5158 (2002).
[18] N. Giovambattista, S. V. Buldyrev, F. W. Starr, and H. E. Stanley, Phys. Rev. Lett. **90**, 085506 (2003).
[19] C. Donati, S. C. Glotzer, P. H. Poole, W. Kob, and S. J. Plimpton, Phys. Rev. E **60**, 3107 (1999).
[20] Y. Gebremichael, M. Vogel, and S. C. Glotzer, J. Chem. Phys. **120**, 4415 (2004).
[21] K. Vollmayr-Lee and A. Zippelius, Phys. Rev. E **72**, 041507 (2005).
[22] H. E. Castillo and A. Parsaeian, Nat. Phys. **3**, 26 (2007).
[23] E. R. Weeks and D. A. Weitz, Phys. Rev. Lett. **89**, 095704 (2002).
[24] F. W. Starr, S. Sastry, J. F. Douglas, and S. C. Glotzer, Phys. Rev. Lett. **89**, 125501 (2002).
[25] T. S. Jain and J. J. De Pablo, J. Chem. Phys. **122**, 174515 (2005).
[26] I. Ladadwa and H. Teichler, Phys. Rev. E **73**, 031501 (2006).
[27] J. C. Conrad, F. W. Starr, and D. A. Weitz, J. Phys. Chem. B **109**, 21235 (2005).
[28] D. N. Perera and P. Harrowell, J. Chem. Phys. **111**, 5441 (1999).
[29] A. Widmer-Cooper, P. Harrowell, and H. Fynewever, Phys. Rev. Lett. **93**, 135701 (2004); A. Widmer-Cooper and P. Harrowell, J. Phys.: Condens. Matter **17**, S4025 (2005).
[30] G. A. Appignanesi, J. A. Rodriguez Fris, and M. A. Frechero, Phys. Rev. Lett. **96**, 237803 (2006).
[31] G. S. Matharoo, M. S. Gulam Razul, and P. H. Poole, Phys. Rev. E **74**, 050502(R) (2006).
[32] P. Charbonneau and D. R. Reichman, Phys. Rev. Lett. **99**, 135701 (2007).
[33] M. I. Mendelev, J. Schmalian, C. Z. Wang, J. R. Morris, and K. M. Ho, Phys. Rev. B **74**, 104206 (2006).
[34] F. Ercolessi and J. B. Adams, Europhys. Lett. **26**, 583 (1994).
[35] X.-Y. Liu, P. P. Ohotnicky, J. B. Adams, C. L. Rohrer, and R. W. Hyland, Surf. Sci. **373**, 357 (1997).
[36] F. C. Frank, Proc. R. Soc. London, Ser. A **215**, 43 (1952).
[37] P. J. Steinhardt, D. R. Nelson, and M. Ronchetti, Phys. Rev. Lett. **47**, 1297 (1981); Phys. Rev. B **28**, 784 (1983).
[38] H. Jonsson and H. C. Andersen, Phys. Rev. Lett. **60**, 2295 (1988).
[39] A. S. Clarke and H. Jonsson, Phys. Rev. E **47**, 3975 (1993).
[40] S. Cozzini and M. Ronchetti, Phys. Rev. B **53**, 12040 (1996).
[41] H. Reichert, O. Klein, H. Dosch, M. Denk, V. Honkimaki, T. Lippmann, and G. Reiter, Nature (London) **408**, 839 (2000).
[42] T. Schenk, D. Holland-Moritz, V. Simonet, R. Bellissent, and D. M. Herlach, Phys. Rev. Lett. **89**, 075507 (2002).
[43] A. Di Cicco, A. Trapananti, S. Faggioni, and A. Filipponi, Phys. Rev. Lett. **91**, 135505 (2003).
[44] W. K. Luo, H. W. Sheng, F. M. Alamgir, J. M. Bai, J. H. He, and E. Ma, Phys. Rev. Lett. **92**, 145502 (2004).
[45] G. W. Lee, A. K. Gangopadhyay, K. F. Kelton, R. W. Hyers, T. J. Rathz, J. R. Rogers, and D. S. Robinson, Phys. Rev. Lett. **93**, 037802 (2004).
[46] K. F. Kelton, G. W. Lee, A. K. Gangopadhyay, R. W. Hyers, T. J. Rathz, J. R. Rogers, M. B. Robinson, and D. S. Robinson, Phys. Rev. Lett. **90**, 195504 (2003).
[47] W. Kob and H. C. Andersen, Phys. Rev. E **51**, 4626 (1995).
[48] J.-P. Hansen and I. R. McDonard, *Theory of Simple Liquids* (Academic, London, 1986).
[49] M. M. Hurley and P. Harrowell, J. Chem. Phys. **105**, 10521 (1996).
[50] A. Rahman, Phys. Rev. **136**, A405 (1964).
[51] W. Pauli, *Thermodynamics and the Kinetic Theory Gases* (MIT, Cambridge, 1973).
[52] B. Doliwa and A. Heuer, Phys. Rev. Lett. **80**, 4915 (1998).
[53] X.-P. Tang, U. Geyer, R. Busch, W. L. Johnson, and Y. Wu, Nature (London) **402**, 160 (1999).
[54] A. Heesemann, V. Zollmer, K. Ratzke, and F. Faupel, Phys. Rev. Lett. **84**, 1467 (2000).
[55] V. Zollmer, K. Ratzke, F. Faupel, A. Rehmet, and U. Geyer, Phys. Rev. B **65**, 220201(R) (2002).
[56] G. A. Appignanesi, J. A. Rodriguez Fris, R. A. Montani, and W. Kob, Phys. Rev. Lett. **96**, 057801 (2006).
[57] G. Adam and J. H. Gibbs, J. Chem. Phys. **43**, 139 (1965); M. Goldstein, *ibid.* **51**, 3728 (1969).